

Optical Properties of the Host Galaxies of Extragalactic Nuclear H₂O Masers

Ingyin Zaw^{1,2}, Guangtun Zhu², Michael Blanton²,
and Lincoln J. Greenhill³

¹New York University Abu Dhabi
P.O. Box 129188, Abu Dhabi, UAE
email: ingyin.zaw@nyu.edu

²Center for Cosmology and Particle Physics, New York University,
4 Washington Place, New York, NY 10003, USA

³Harvard-Smithsonian Center for Astrophysics 60 Garden St.,
Cambridge, MA 02138, USA

Abstract. Although most nuclear 22GHz ($\lambda = 1.35$ cm) H₂O masers are in Seyfert 2 and LINER galaxies, only a small fraction of such galaxies host water masers. We systematically study the optical properties of the galaxies with and without nuclear H₂O maser emission to better understand the relationship between H₂O maser emission and properties of the central supermassive black hole and improve the detection rates in future surveys. To this end, we cross-matched the galaxies from H₂O maser surveys, both detections and non-detections, with the Sloan Digital Sky Survey (SDSS) low-redshift galaxy sample. We find that maser detection rates are higher at higher optical luminosity (M_B), larger velocity dispersion (σ), and higher [O III] $\lambda 5007$ luminosity, with [O III] $\lambda 5007$ being the dominant factor, and that the isotropic maser luminosity is correlated with these variables. These correlations are natural if maser emission depends on the host SMBH mass and AGN activity. We also find that the detection rate is higher for galaxies with higher extinction. These results indicate that, by pre-selecting galaxies with high extinction-corrected [O III] $\lambda 5007$ flux, future maser surveys can increase detection efficiencies by a factor of ~ 3 to ~ 5 .

Keywords. masers, galaxies: active, galaxies: nuclei, galaxies: Seyfert, radio lines: galaxies

1. Introduction

Water maser emission at 22 GHz ($\lambda = 1.35$ cm) has been mainly associated with active galactic nuclei (AGNs) and is currently the only resolvable tracer of warm, dense molecular gas in the inner parsec of AGNs. These masers are found in a variety of regions, such as jets/winds and nearly edge-on, rotating accretion disks. The latter, “disk masers”, have been used to measure many properties of the central engine, including accurate SMBH masses (e.g. Kuo *et al.* 2011), accretion disk geometry (e.g. Greenhill *et al.* 2003), and geometric distances to host galaxies (e.g. Humphreys *et al.* 2008, Braatz *et al.* 2010). Unfortunately, these extragalactic nuclear H₂O masers are extremely rare. Discovering what sets maser host galaxies apart from other AGNs would lead not only to a better understanding of the connections between H₂O maser emissions and the properties of the AGN but also make surveys more efficient.

Earlier studies have found that most H₂O masers are found in Seyfert 2’s and LINERS (instead of Seyfert 1’s) (e.g. Braatz *et al.* 1997, Kondratko *et al.* 2006b) and that maser emission is more likely in systems with high X-ray obscuring columns (e.g. Madejski *et al.* 2006, Zhang *et al.* 2006, Greenhill *et al.* 2003, Zhang *et al.* 2010). Correlations have also been reported between H₂O maser isotropic luminosity and 2-10 keV X-ray

luminosity (Kondratko *et al.* 2006a) and far IR luminosity (Henkel *et al.* 2005). However, there are currently no large samples of AGNs with measured 2–10 keV X-ray luminosities, and a high far IR luminosity does not guarantee that the galaxy will also be an AGN. Although most H₂O masers are in Seyfert 2's and LINERs, most Seyfert 2's and LINERs do not have maser emission. Since maser surveys may start with a sample of Seyfert 2's and LINERs, they are already targeting galaxies with optical spectra. In addition, there exist large optical surveys, such as the Sloan Digital Sky Survey (SDSS), 2dF Galaxy Redshift Survey (2dFGRS) and 6dF Galaxy Survey (6dFGS). Consequently, if masers can be shown to be in galaxies with certain optical properties, large maser surveys can select targets based on these properties. We systematically studied the optical properties of the maser hosts and known non-detections by cross-matching the SDSS low-redshift galaxy catalog with all galaxies surveyed for maser emission. The results are presented in later sections and further details can be found in Zhu *et al.* 2011.

2. Galaxy Samples and Optical Property Selection

For a full sample of maser detections and non-detections, we combine the catalogs (as of 1 Dec. 2010) on the Megamaser Cosmology Project (MCP[†]) and Hubble Constant Maser Experiment (HoME[‡]) web sites. In order to restrict ourselves to masers associated with AGNs, we exclude the galaxies associated with star formation regions, as noted in the MCP or HoME catalogs. We also construct a master list of non-detections listed by MCP and HoME and remove duplicates. This resulted in a total of 123 known masers, of which ~40 are noted as disk masers on the HoME web site based on very long baseline interferometry (VLBI) maps or single-dish spectra, and 3806 non-detections, for an overall detection rate of ~3%.

The SDSS Data Release 7 (DR7; Abazajian *et al.* 2009) catalog provides a complete sample of galaxies with uniform imaging and spectroscopy to systematically study optical properties related to maser emission. Since the masers are mostly nearby and the SDSS photometry and spectroscopy samples are most complete at low redshifts, we limit ourselves to galaxies with $z < 0.05$ (excluding only 4 maser galaxies). For photometry, we use the low- z catalog from the NYU Value Added Galaxy Catalog (NYU-VAGC; Blanton *et al.* 2005) and for spectroscopic parameters, we use the measurements of the MPA-JHU group[¶] (e.g. Tremonti *et al.* 2004). We cross-match this SDSS low- z sample with maser detections and non-detections. We find 48 detections (15 disk masers) and 1588 non-detections which have SDSS photometry, of which 33 detections (10 disk masers) and 1030 non-detections have well measured spectral properties. The detection rates in both the photometric and spectroscopic samples are ~3%. This is similar to the total sample, and therefore, the cross-matching should not cause a bias for the analysis of optical properties of maser host galaxies.

SDSS provides a plethora of photometric and spectroscopic measurements. We choose to study the following properties based on the assumption that maser emission should be related to properties of the central SMBH: [O III] $\lambda 5007$ luminosity ($L_{[\text{O III}]\lambda 5007}$, in erg s^{-1}), a well-known bolometric luminosity indicator (Heckman *et al.* 2005), and velocity dispersion (σ , in km s^{-1}), correlated with SMBH mass (Ferrarese *et al.* 2000). Since [O III] $\lambda 5007$ can be obscured by the material in the host galaxy and we expect masers to be in systems with high obscuration, we also look at the Balmer decrement, $H\alpha/H\beta$, and correct the observed [O III] $\lambda 5007$ luminosity, $L_{[\text{O III}]\lambda 5007, \text{obs}}$, to obtain the

[†] <https://safe.nrao.edu/wiki/bin/view/Main/MegamaserCosmologyProject>

[‡] <https://www.cfa.harvard.edu/~lincoln/demo/HoME/index.html>

[¶] <http://www.mpa-garching.mpg.de/SDSS/DR7/>

intrinsic [O III] $\lambda 5007$ luminosity, $L_{[\text{OIII}]\lambda 5007, \text{cor}}$. Finally, we study B band magnitude, M_B , as an indicator of optical luminosity.

3. Results

We find that maser detection rates depend on the optical properties of host galaxies. The strongest effect is that detection rates are higher for higher [O III] $\lambda 5007$ luminosity. Detection rates are also higher for galaxies with higher $H\alpha/H\beta$, and consequently, the extinction-corrected [O III] $\lambda 5007$ luminosity, $L_{[\text{OIII}]\lambda 5007, \text{cor}}$, distribution for maser host galaxies and non-detections are even more discrepant than for observed [O III] $\lambda 5007$ luminosity, $L_{[\text{OIII}]\lambda 5007, \text{obs}}$. Figure 1 shows the distributions of $L_{[\text{OIII}]\lambda 5007, \text{obs}}$, $L_{[\text{OIII}]\lambda 5007, \text{cor}}$, and $H\alpha/H\beta$ for maser hosts and non-detections as well as the detection rates with respect to these variables.

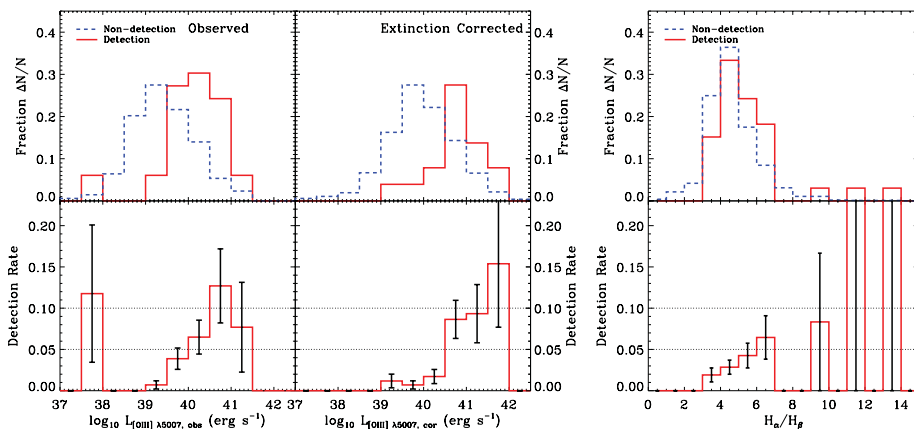


Figure 1. $L_{[\text{OIII}]\lambda 5007, \text{cor}}$, $L_{[\text{OIII}]\lambda 5007, \text{obs}}$, and Balmer decrement. The top panels show the distributions for maser detections (blue) and non-detections (red). The bottom panels show the detection rate as a function of these optical properties.

As shown in Figure 2, maser detection rates are also higher for higher B band magnitude, M_B , and velocity dispersion, σ . We denote the disk masers with green diamonds but, due to the smallness of the sample, we do not draw conclusions just based on the disk masers. Although weaker than the dependence on $L_{[\text{OIII}]\lambda 5007}$, the dependence of detection rates on M_B and σ persist even for galaxies with high $L_{[\text{OIII}]\lambda 5007}$ (Zhu *et al.* 2011).

We test whether the dependence of detection rate on $L_{[\text{OIII}]\lambda 5007}$, σ , and M_B is a consequence of an underlying correlation between these properties and maser luminosity. We collected 66 isotropic maser luminosities from literature (see table in Zhu *et al.* 2011). The left panel in Figure 4 shows the isotropic H_2O maser luminosity against redshift. The plot shows a flux-limited effect, with a maximum sensitivity of $\sim 0.1 \text{ Jy km s}^{-1}$, similar to the sensitivities of surveys with the Green Bank Telescope (GBT) (e.g. Braatz *et al.* 2004). This is consistent with earlier findings that detection rates are higher for galaxies with smaller recession velocities (e.g. Braatz *et al.* 1997). We compare the isotropic luminosity with our optical properties of interest. We note that isotropic luminosity is not ideal for several reasons, e.g. maser emission is beamed and variable and that isotropic luminosities are from different observations with different sensitivities. In addition, we have supplemented our SDSS sample with measurements from literature to increase the sample size. All these effects will add scatter. Despite these shortcomings,

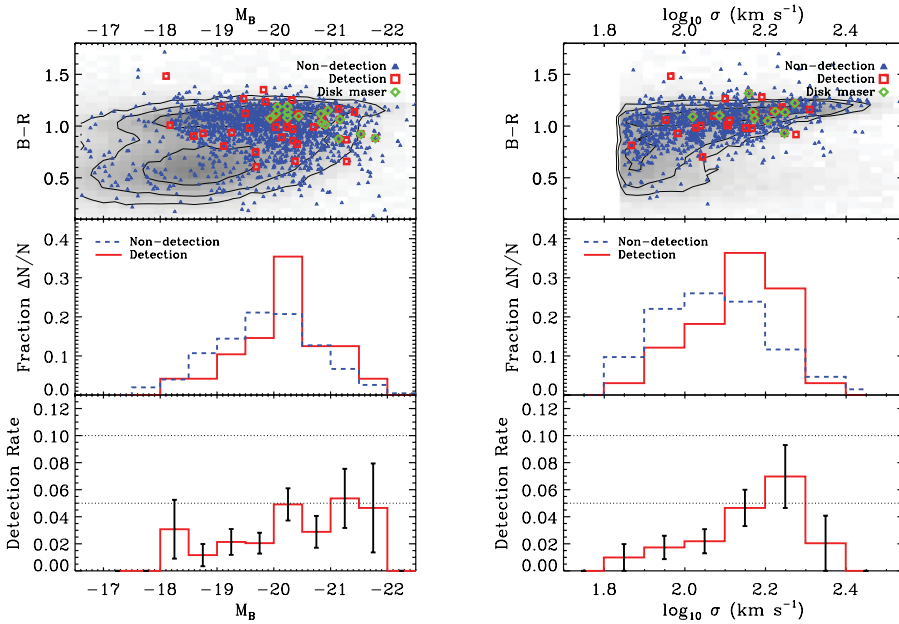


Figure 2. *B* band magnitude (left) and velocity dispersion, σ (right). Top panels show the color-magnitude diagrams with the full low-*z* photometric sample in grayscale, with contours representing 40%, 80%, and 90% of the sample. Middle panels show the distributions of these variables, and the bottom panels show the detection rate as a function of these variables.

we find that isotropic maser luminosity is correlated with $L_{[\text{OIII}]\lambda 5007, \text{cor}}$, $L_{[\text{OIII}]\lambda 5007, \text{obs}}$, σ , and M_B , albeit with large scatter, as shown in Figure 3. Larger samples are needed to further test these correlations and whether the correlations depend on maser environment (e.g. jets vs. disks).

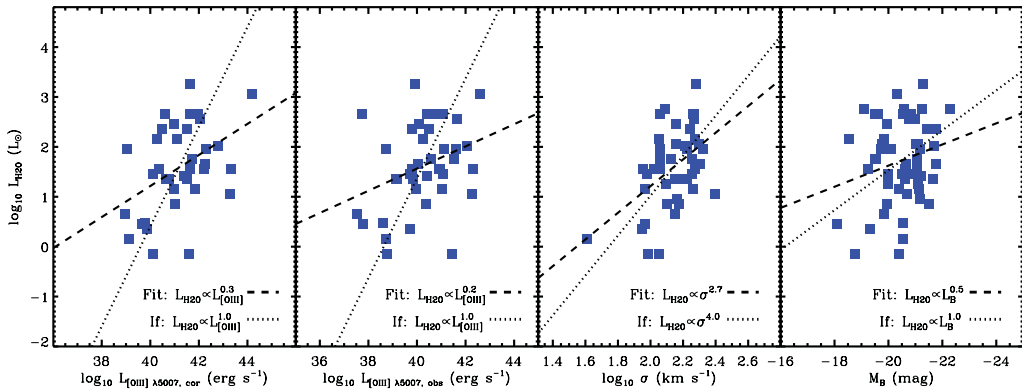


Figure 3. Relations between isotropic maser luminosity ($L_{\text{H}2\text{O}}$) and $L_{[\text{OIII}]\lambda 5007, \text{cor}}$, $L_{[\text{OIII}]\lambda 5007, \text{obs}}$, σ , and M_B of the host galaxies. The dashed lines are the linear least-squares fits assuming a uniform error of 0.5 dex in $\log_{10} L_{\text{H}2\text{O}}$. The dotted lines show the linear least-squares fits with the slopes fixed assuming that $L_{\text{H}2\text{O}} \propto L_{\text{AGN}} \propto M_{\text{BH}}$, and $M_{\text{BH}} \propto L_B \propto \sigma^4$, and $L_{\text{AGN}} \propto L_{[\text{OIII}]\lambda 5007}$.

4. Discussion and Recommendations for Future Surveys

The correlations we see between isotropic maser luminosity with $L_{[\text{O III}]\lambda 5007, \text{cor}}$, $L_{[\text{O III}]\lambda 5007, \text{obs}}$, σ , and M_B would be natural if the strength of maser emission depends on AGN activity and SMBH mass. We fit these results to a simplified model in which we assume $L_{\text{H}_2\text{O}} \propto L_{\text{AGN}} \propto M_{\text{BH}}$, $M_{\text{BH}} \propto L_B \propto \sigma^4$, and $L_{\text{AGN}} \propto L_{[\text{O III}]\lambda 5007}$ (see Zhu *et al.* 2011 for rationale). Using the intercepts from the fits, we translate the survey maser isotropic luminosity flux limit to corrected and observed [O III] $\lambda 5007$ luminosity limits which are plotted against redshift in the right panel of Figure 4. If surveys are limited to the galaxies with high $L_{[\text{O III}]\lambda 5007}$, the detection rates could be improved by a factor of ~ 3 (for $L_{[\text{O III}]\lambda 5007, \text{obs}}$) to ~ 5 (for $L_{[\text{O III}]\lambda 5007, \text{cor}}$). Even if surveys do not cut on $L_{[\text{O III}]\lambda 5007}$, the galaxies should be ranked by $L_{[\text{O III}]\lambda 5007}$ so that discoveries are front-loaded. If $L_{[\text{O III}]\lambda 5007}$ is unavailable, surveys should rank galaxies by velocity dispersion or by optical luminosity.

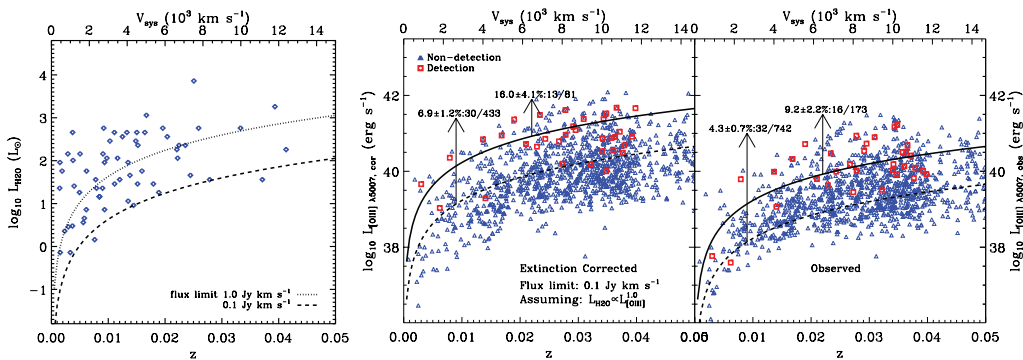


Figure 4. H_2O maser isotropic luminosity (left) and extinction-corrected [O III] $\lambda 5007$ luminosity, $L_{[\text{O III}]\lambda 5007, \text{cor}}$, and observed [O III] $\lambda 5007$ luminosity, $L_{[\text{O III}]\lambda 5007, \text{obs}}$ (right), as a function of redshift. The solid lines indicate a maser flux limit of 0.1 Jy km s^{-1} and the dashed lines are the flux limit shifted downward by -1.0 dex. The arrows and percentages are detection rates above the corresponding lines.

References

- Abazajian K. N., Adelman-McCarthy, J. K., Agueros, M. A., *et al.* 2009, *ApJS*, 182, 543
 Blanton, M. R., Schlegel, D. J., Strauss, M. A., *et al.* 2005, *AJ*, 129, 2562
 Braatz, J. A., Wilson, A. S., & Henkel, C. 1997, *ApJS*, 110, 321
 Braatz, J. A., Henkel, C., Greenhill, L. J., Moran, J. M., & Wilson, A. S. 2004, *ApJ*, 617, L29
 Braatz, J. A., Reid, M. J., Humphreys, E. M. L., *et al.* 2010, *ApJ*, 718, 657
 Ferrarese, L. & Merritt, D. 2000, *ApJ*, 539, L9
 Greenhill, L. J., Booth, R. S., Ellingsen, S. P., *et al.* 2003, *ApJ*, 590, 162
 Greenhill, L. J., Tilak, A., & Madejski, G. 2008, *ApJ*, 686, L13
 Heckman, T. M., Ptak, A., Hornschemeier, A., Kauffmann, G., *et al.* 2005, *ApJ*, 643, 161
 Henkel, C., Braatz, J. A., Tarchi, A., *et al.* 2005, *Ap&SS*, 295, 107
 Humphreys, E. M. L., Reid, M. J., Greenhill, *et al.* 2008, *ApJ*, 672, 800
 Kondratko, P. T., Greenhill, L. J., & Moran, J. M. 2006a, *ApJ*, 652, 138
 Kondratko, P. T., Greenhill, L. J., Moran, J. M., *et al.* 2006b, *ApJ*, 638, 100
 Kuo, C. Y., Braatz, J. A., Condon, J. J., *et al.* 2011, *ApJ*, 727, 20
 Madejski, G., Done, C., Zycki, P. T., & Greenhill, L. 2006, *ApJ*, 636, 75
 Tremonti, C. A., Heckman, T. M., Kauffmann, G., *et al.* 2004, *ApJ*, 613, 898
 Zhang, J. S., Henkel, C., Kadler, M., *et al.* 2006, *A&A*, 450, 933
 Zhang, J. S., Henkel, C., Guo, Q., Wang, H. G., & Fan, J. H. 2010, *ApJ*, 708, 1528
 Zhu, G., Zaw, I., Blanton, M. R., & Greenhill, L. J. 2011, *ApJ*, 742, 73